The *Drosophila* SWI/SNF chromatin-remodeling complexes play separate roles in regulating growth and cell fate during regeneration

Short title: The SWI/SNF chromatin-remodeling complexes regulate regeneration

Yuan Tian[1] and Rachel K. Smith-Bolton[1*]

[1]Department of Cell and Developmental Biology, University of Illinois at Urbana-Champaign,

Urbana, IL, USA

*Correspondence: rsbolton@illinois.edu

Abstract

Regeneration is a precise process that requires regulated cell proliferation and accurate cell fate decisions. The mechanisms that temporally and spatially control the activation or repression of important genes during regeneration are not fully understood. Epigenetic modification of regeneration genes by Polycomb group and Trithorax group chromatin regulators could be key factors that govern gene repression and activation in damaged tissue. Here we report a genetic screen of chromatin regulators that identified phenotypes for many PcG and TrxG mutants and RNAi lines in *Drosophila* imaginal wing disc regeneration. Furthermore, we show that the two *Drosophila* SWI/SNF chromatin-remodeling complexes, BAP and PBAP, play distinct roles in regeneration. The PBAP complex regulates regenerative growth and developmental timing, and is required for the expression of JNK signaling targets and upregulation of the growth promoter *myc*. By contrast, the BAP complex is required for ensuring proper patterning and cell fate by stabilizing expression of the posterior gene *engrailed*. The core complex components are required for both processes: a weak knockdown of *brahma* (*brm*), which encodes the only ATPase of the SWI/SNF complexes, induces the BAP mutant regeneration phenotype, whereas a strong *brm* mutant shows the PBAP regeneration phenotype. Thus, both SWI/SNF complexes are essential for proper gene expression

during tissue regeneration, but play distinct roles in regulating growth and cell fate.

Author summary

To regenerate, damaged tissue must heal the wound, regrow to the proper size, replace the correct cell types, and return to the normal gene expression program. Such dramatic changes in cellular and tissue behavior require rapid and accurate changes of gene expression. Chromatin modifiers are likely to play a role in regulating these changes in gene expression. We induced ablation in *Drosophila* imaginal wing discs using genetic tools, and performed a genetic screen for chromatin modifiers that regulate epithelial tissue regeneration. Here we show that many Polycomb and Trithorax Group genes are indeed important for promoting or constraining regeneration. Specifically, the two SWI/SNF chromatin-remodeling complexes play distinct roles in regulating different aspects of regeneration. The PBAP complex regulates expression of JNK signaling targets, thereby controlling growth and developmental timing, while the BAP complex prevents damage-induced cell fate changes in the posterior compartment of the wing.

Introduction

Regeneration is a complex yet highly elegant process that some organisms can

use to recognize, repair and replace missing tissue. Imaginal disc repair in *Drosophila* is a good model system for understanding regeneration due to the high capacity of these tissues to regrow and restore complex patterning information, and the genetic tools available in this model organism [1]. Regeneration requires the coordinated expression of genes that regulate the sensing of tissue damage, induction of regenerative growth, re-patterning of the tissue, and coordination of regeneration with developmental timing to end the process. However, how regeneration genes are regulated is not fully understood.

Regulation of gene expression through changes in chromatin structure is essential in many biological processes [2–4]. Chromatin structure can be regulated by histone modifications and by ATP-dependent chromatin remodeling [5]. Recently, several chromatin remodelers have been identified as important for regeneration in different model organisms, suggesting that they regulate gene expression during this process. For example, Brahma (Brm), the ATPase of the SWItch/Sucrose Non-Fermentable (SWI/SNF) chromatin remodeling complexes, is required for *Drosophila* midgut regeneration [6]. Brg1, a mammalian homolog of Brm, is indispensable for the control of bulge stem cells during mouse skin regeneration [7]. Deletion of the SWI/SNF component *Arid1a* improves tissue repair in the mouse liver and ear without causing tumor formation [8]. In addition, specific components of

the Nucleosome Remodeling and Deacetylase (NuRD) complex are expressed in the regeneration blastema and are required for caudal fin regeneration in zebrafish [9]. The planarian gene *Smed-CHD4*, which is the homolog of Mi-2, the ATP-dependent engine of the NuRD complexes, is essential for planarian regeneration because it is required for neoblast differentiation [10]. Furthermore, a number of genes associated with chromatin remodeling showed transcriptional level changes during late-stage regeneration after *Drosophila* wing disc fragmentation, including *bap60* and *bap111,* which are SWI/SNF complexes members [11]. Importantly, the aspects of regeneration controlled by many of these chromatin remodelers and their genetic targets are not known.

Histone modification genes have also been implicated in regulation of regeneration. For example, pharmacological blockade of Histone Deacetylase (HDAC) activity inhibits Xenopus tadpole tail regeneration [12]. Bmi1, a PRC1 complex member, is upregulated during and is required for regeneration of the exocrine pancreas in mice [13]. Kdm6b.1, an H3K27 demethylase, is required for zebrafish fin regeneration [14]. HDAC1 cooperates with C/EBP to regulate termination of mouse liver regeneration [15]. C/EBPα-Brm-HDAC1, a multi-protein complex, silences E2F-dependent promoters, reducing regenerative ability in old mouse livers [16]. In *Drosophila* wing disc regeneration, *ash2*, which is a Trithorax group member, showed

changes in transcription levels during late-stage regeneration [11], the histone methylase Trithorax (Trx) regulates Jun N-terminal kinase (JNK) signaling via the phosphatase *puckered* (*puc*) [17], and the gene *wingless* has a damage-responsive enhancer that is activated specifically after tissue damage in younger animals, but is silenced through H3K27 methylation deposited by the PRC2 complex in older animals [18]. These studies demonstrated the importance of chromatin modification in regeneration. However, little is known about how these proteins control gene regulatory networks during regeneration and how they are regulated and targeted after tissue damage.

To probe the role of chromatin modifiers in tissue regeneration more systematically, we assembled and screened a collection of pre-existing *Drosophila* Polycomb Group (PcG) and Trithorax Group (TrxG) mutants for regeneration defects using the *Drosophila* wing imaginal disc. We used a spatially and temporally controllable tissue-ablation method that uses transgenic tools to induce tissue damage only in the wing primordium [19]. This powerful system ablates 94% of the wing primordium on average at the early third instar and allows the damaged wing discs to regenerate *in situ*. Genes regulating different aspects of regeneration, such as *taranis*, *trithorax*, and *cap-n-collar*, were identified through our previous forward genetic screens using this tissue ablation method [17,20,21].

Through the targeted genetic screen of chromatin regulators presented here we found that mutants in several of the *Drosophila* SWI/SNF components showed interesting regeneration defects. We show that the SWI/SNF complexes BAP and PBAP are required for regeneration, and that the two complexes play distinct roles. Previously, our lab identified a gene, *taranis*, that is required for maintaining posterior cell fate in regenerating *Drosophila* wing imaginal discs [20]. Here we show that the BAP complex functions to preserve posterior cell fate after wounding in parallel to Taranis. By contrast, the PBAP complex is important for the activation of JNK signaling targets, including expression of *myc* to drive regenerative growth, and *dilp8* to delay metamorphosis and allow enough time for the damaged tissue to regrow.

Results

A genetic screen of chromatin modifier mutants

To identify regeneration genes among *Drosophila* PcG and TrxG members, we conducted a genetic screen similar to our previously reported unbiased genetic screen for genes that regulate wing imaginal disc regeneration [21] using existing mutants or RNAi lines of chromatin modifiers (Fig 1A). To induce tissue ablation, *rotund-GAL4* drove the expression of the pro-apoptotic gene *UAS-reaper* in the

imaginal wing pouch, and *tubulin-GAL80^{ts}* provided temporal control, enabling us to turn ablation on and off by varying the temperature [19]. The ablation was carried out for 24 hours during the early third instar. We characterized the quality of regeneration by assessing the adult wing size, and identifying patterning defects by scoring ectopic or missing features. The size of the regenerated adult wings was assessed semi-quantitatively, by counting the wings that were approximately 0%, 25%, 50%, 75%, or 100% of the length of a control adult wing. Using this system, we screened populations of animal with the genotypes listed in S1 Table.

Eighty percent of the PcG and TrxG mutants and RNAi lines tested had a change in regeneration index of 10% or more compared to controls (see materials and methods for regeneration index calculation) (S1 Table), consistent with the idea that changes in chromatin structure are required for the damaged tissue to execute the regeneration program. Importantly, these genotypes did not show obvious defects in adult wings after normal development (data not shown). Thus, regenerating tissues are more sensitive to reduced levels of PcG and TrxG genes. Flies heterozygous mutant for a majority of PcG members had larger adult wings after ablation and regeneration compared to control *w^{1118}* animals that had also regenerated, indicating that reducing PcG levels enhanced regeneration. These results suggest that pro-regeneration genes may normally be repressed by the PcG chromatin

modifications. Interestingly, some TrxG mutants or RNAi lines had smaller adult wings after damage and regeneration, indicating that loss of these genes impaired regeneration, while other TrxG mutants had larger wings after regeneration. This variation in phenotypes among the TrxG mutants may be due to the broad range of functions that TrxG proteins have, including histone modification and chromatin remodeling, which can result in either gene activation or repression [22]. Interestingly, mutants of different components in the same complex, such as the PRC2 complex and the SWI/SNF complexes, had different phenotypes.

The PBAP Complex Is Required for Regenerative Growth, while the BAP Complex Is Required for Posterior Cell Fate

The SWI/SNF complexes are conserved multi-subunit protein complexes that activate or repress gene expression [22] by using the energy from ATP hydrolysis to disrupt histone-DNA contacts and remodel nucleosome structure and position [23,24]. Brm is the only ATPase of the SWI/SNF complexes in *Drosophila* [25]. Other components contain domains involved in protein-protein interactions, protein-DNA interactions, or interactions with modified histones [26]. There are two subtypes of SWI/SNF in *Drosophila*: the Brahma-associated proteins (BAP) and the Polybromo-associated BAP (PBAP) remodeling complexes [25,27]. They share common core components, including Brm, Snr1, Moira (Mor), Bap55, Bap60,

Bap111 and Actin [25], but contain different signature proteins. The PBAP complex is defined by the components Bap170, Polybromo and Sayp [25,28]. Osa defines the BAP complex [29,30].

As shown in S1 Table, different components of the SWI/SNF complexes showed different phenotypes after ablation and regeneration of the wing pouches. Animals heterozygous mutant for the PBAP-specific component Bap170 (*bap170*$^{\Delta 135}$/+) had adult wings that were smaller after disc regeneration than *w*^{1118} adult wings after disc regeneration (Fig 1B). Thus, Bap170 is required for regeneration, suggesting that the PBAP complex is required for ablated wings to regrow.

By contrast, animals heterozygous mutant for the BAP-specific component Osa (*osa*^{308}/+) had adult wings that were larger than *w*^{1118} adult wings and showed severe patterning defects after damage and regeneration of the disc (Fig 1C-1E). Specifically, the posterior compartment of the *osa*^{308}/+ wings had anterior features after damage and regeneration of the disc, but had normal wings when no tissue damage was induced. To quantify the extent of the posterior-to-anterior (P-to-A) transformations, we quantified the number of anterior features in the posterior of each wing, including socketed bristles and ectopic veins on the posterior margin, an ectopic anterior crossvein (ACV), costal bristles on the alula, and an altered

shape that has a narrower proximal and wider distal P compartment[20] (Fig 1F). While w^{1118} adult wings that had regenerated as discs had a low level of P-to-A transformations induced by JNK signaling [20], 75% of the osa^{308}/+ wings had P-to-A transformations, and 83% of these transformed wings had 4 or 5 anterior markers in the posterior, representing extensive posterior compartment transformations. Thus, Osa is required to preserve posterior cell fate during regeneration, suggesting that the BAP complex regulates cell fate after damage.

To identify when the P-to-A transformations happen, we examined the expression of anterior- and posterior-specific genes during tissue regeneration. Regenerating wing discs were dissected out at different times during recovery (R). At 72 hours after damage (R72), in osa^{308}/+ regenerating discs, the posterior selector gene *engrailed* (*en*) was expressed in the posterior compartment, but lost in patches (Fig 2A and 2B). In addition, the proneural protein Acheate (Ac), which is expressed in sensory organ precursors in the anterior of wing discs [31], was ectopically expressed in the posterior (Fig 2C and 2D) marking likely precursors to the socketed bristles found in the posterior of the adult wings. The anterior genes *cubitus interruptus* (*ci*) [32] and *patched* (*ptc*) [33] were ectopically expressed in the posterior of the osa^{308}/+ R72 regenerating wing discs (Fig 2E and 2F). The ectopic expression of these anterior genes was not observed at R48, suggesting that the

P-to-A fate transformations happened late during regeneration (Fig 2G and 2H). This phenotype is similar to that of *taranis* (*tara*) heterozygous mutants during regeneration [20]. Tara prevents P-to-A cell fate transformations induced by elevated JNK signaling during regeneration. Thus, the BAP-specific component *osa,* and likely the BAP complex itself, may work with Tara to preserve posterior fate during the later stages of regeneration.

The increased wing size after regeneration in osa^{308}/+ animals was likely a secondary result of the patterning defect, as ectopic *ptc* and *ci* expression correlates with ectopic AP boundaries that stimulate excess growth [20]. Furthermore, pupariation occurred later in osa^{308}/+ regenerating animals compared to w^{1118} regenerating animals (S1A and S1B Fig), which provided more time for regeneration in the mutant animals.

The roles of the SWI/SNF chromatin remodeling complexes are specialized in different tissues during development [34,35,26]. Importantly, during development BAP regulates growth in the *Drosophila* wing disc [34], suggesting that the roles of the SWI/SNF complexes in regeneration are distinct from their roles in normal development.

Reducing levels of the core SWI/SNF component Brahma to different levels shows either poor regeneration or P-to-A transformations

Because mutants of BAP or PBAP complex-specific components showed distinct phenotypes, we screened mutants of the core components for regeneration phenotypes. Assuming the core components are required for both complexes, we expected their mutants to have small wings after disc regeneration like the *bap170*/+ animals. We also expected that AP patterning would be disrupted, but it was not possible to assess AP patterning in these small wings because patterning was incomplete. Interestingly, mutants or RNAi lines that reduced levels of the core components were split between the two phenotypes. For example, brm^{2}/+ discs and discs expressing a *bap111* RNAi construct regenerated poorly, resulting in small wings, while $bap55^{LL05955}$/+ discs, mor^{1}/+ discs, and discs expressing a *bap60* RNAi construct showed P-to-A transformations in the adult wings and larger wings overall after damage and regeneration of the discs (Fig 3A-3G).

There are two possible explanations for why some core components lacked a regenerative growth phenotype. One possibility is that the SWI/SNF complex components assemble in a unique way during regeneration, and these “core” components are unnecessary for the complex that regulates regenerative growth. This scenario is unlikely, as any SWI/SNF complex should require the function of the

scaffold Mor [36]. Another possibility is that some of the mutants and RNAi lines caused partial loss of function, which impaired the BAP complex but did not impair the PBAP complex.

To test this second possibility, we used a strong mutant and a weak RNAi line to reduce the gene function of the core component *brm*. brm^{2} is an amorphic allele generated through ethyl methanesulfonate mutagenesis [37]. brm^{2}/+ animals showed the small wing phenotype indicating poor regeneration (Fig 3A), similar to the PBAP complex-specific $bap170^{\Delta 135}$/+ mutants. By contrast, knockdown of *brm* by expressing a *brm* RNAi construct during tissue ablation induced P-to-A transformations, similar to the BAP complex-specific osa^{308}/+ mutants (Fig 3H). At R72, 80% of the *brm* RNAi wing discs had ectopic expression of the anterior genes *ptc* and *ci* in the posterior of the discs (n=10), while no expression of *ptc* or *ci* was observed in the posterior of control R72 discs (n=10) (Fig 3I and 3J). Thus, reducing the core SWI/SNF component Brm to different levels produced one or the other phenotype. We propose that decreasing Brm levels via RNAi caused the loss of BAP function and misregulation of cell fate, while decreasing Brm function via the strong mutation resulted in the loss of PBAP function, resulting in small wing size after disc regeneration.

The PBAP complex is required for Myc upregulation and cell proliferation during regrowth

To identify when the defect in regrowth occurs in PBAP complex mutants, we measured the regenerating wing pouch in w^{1118} controls, $bap170^{\Delta 135}$/+ and brm^{2}/+ mutants, as well as in the osa^{308}/+ BAP mutant for comparison. The $bap170^{\Delta 135}$/+ regenerating wing pouches were smaller than w^{1118} at 36 hours after tissue damage (Fig 4A-4C). brm^{2}/+ mutant animals also had smaller regenerating wing pouches during regeneration (S1C-E Fig). By contrast, the regenerating osa^{308}/+ wing pouches regrew at the same rate as controls (S1F-J Fig).

To determine whether the $bap170^{\Delta 135}$/+ mutant animals had a slower rate of proliferation, we quantified the number of mitotic cells in the regenerating wing pouch. A significant decrease in the number of PH3-positive cells was observed in $bap170^{\Delta 135}$/+ mutants (Fig 4D-4F, S1K Fig). While smaller adult wings could also be caused by increased cell death in the regenerating tissue, we did not find an increase in cell death in the brm^{2}/+ discs, as marked by immunostaining for cleaved Caspase 3 (S1L and S1M Fig).

To identify why proliferation is slow in $bap170^{\Delta 135}$/+ mutants, we examined levels of Myc, an important growth regulator that is upregulated during *Drosophila* wing

disc regeneration[19]. In mammals, *c-myc* is a direct target of the SWI/SNF (BAP) complex[38], but a role for the PBAP complex in regulating the *myc* gene has not been established. Myc levels were significantly reduced in *bap170*$^{\Delta 135}$/+ and *brm*^{2}/+ regenerating discs compared to wild-type regenerating discs (Fig 4G-4I and S1N-P Fig). By contrast, there was no change in Myc levels in *osa*^{308}/+ mutants (S1Q-S Fig).

The PBAP complex is required for the delay in pupariation induced by tissue damage

Damaged imaginal discs delay pupariation by expressing ILP8, which delays the production of ecdysone and onset of metamorphosis, providing more time for damaged tissue to regenerate [39,40]. To determine whether the SWI/SNF complexes regulate the timing of metamorphosis, we quantified the pupariation rate in *w*^{1118} and *bap170*$^{\Delta 135}$/+ regenerating animals. Without tissue damage, *bap170*$^{\Delta 135}$/+ mutants pupariated slightly later than *w*^{1118} animals (Fig 4J). However, after wing disc damage, *bap170*$^{\Delta 135}$/+ mutants pupariated earlier than *w*^{1118} animals by about one day, which means the mutants had less time for regeneration (Fig 4K). To uncover why *bap170*$^{\Delta 135}$/+ animals had less regeneration time, we quantified *ilp8* transcription levels. qPCR data revealed that *bap170*$^{\Delta 135}$/+ animals had about 50% less *ilp8* mRNA (Fig 4L).

The PBAP complex regulates expression of JNK signaling targets

SWI/SNF complexes can be recruited by transcription factors to act as co-activators of gene expression[41]. Regenerative growth and the pupariation delay are regulated by JNK signaling [39,40,42,43]. Thus, it is possible that PBAP is recruited to JNK signaling targets like *ilp8* by the AP-1 transcription factor [44]. To determine whether *bap170* is required for JNK-dependent transcription, we examined the activity of the TRE-Red reporter, which is composed of four AP-1 binding sites (TREs) driving the expression of a DsRed.T4 reporter gene [45] in w^{1118} and $bap170^{\Delta 135}$/+ regenerating wing discs. The TRE-Red intensity was significantly decreased in the $bap170^{\Delta 135}$/+ regenerating tissue compared to the w^{1118} regenerating tissue (Fig 4M-4O), indicating that PBAP is required for full activation of gene expression by AP-1 and JNK signaling.

The BAP complex does not regulate JNK signaling

JNK signaling can alter cell fate during regeneration by perturbing *en* expression, and Tara counters the effects of JNK activity by stabilizing *en* expression [20]. Thus, BAP complex mutations might cause P-to-A transformations by elevating JNK signaling, by reducing *tara* expression, or by misregulating *en* directly. To determine whether the BAP complex regulates JNK signaling, we examined the JNK reporter

TRE-Red and immunostaining for phosphorylated, activated JNK in *osa*^{308}/+ and *w*^{1118} regenerating wing discs. TRE-Red intensity was not different between *osa*^{308}/+ and *w*^{1118} regenerating tissue (Fig 5A-5C), nor was phospho-JNK immunostsaining (S2A and S2B Fig). Thus, the BAP complex acts to protect posterior cell fate downstream of or in parallel to JNK signaling.

The BAP complex functions in parallel to Taranis to preserve cell fate

Because *tara* is regulated transcriptionally after tissue damage [20], we examined whether the BAP complex is required for *tara* upregulation. Using a *tara-lacZ* enhancer-trap, we assessed expression in *bap55*^{LL05955}/+ regenerating wing discs, which had the same P-to-A transformations as the *osa*^{308}/+ regenerating discs. No change in *tara-lacZ* expression was identified, (Fig 5D-5F), indicating that the damage-dependent *tara* expression was not downstream of BAP activity.

To determine whether Tara can suppress the P-to-A transformations induced by the reduction of Osa, we overexpressed Tara using *UAS-tara* under control of *rn-Gal4* in the *osa*^{308}/+ mutant animals, generating elevated Tara levels in the *rn*-expressing cells that survived the tissue ablation. Indeed, the P-to-A transformation phenotype in *osa*^{308}/+ mutant animals was rescued by Tara overexpression (Fig

5G-5J). Furthermore, Osa protein levels did not appear to change during regeneration and were unchanged in *tara*^{1}/+ mutant regenerating discs (S2C and S2D Fig), suggesting that Tara does not regulate *osa* expression, and the BAP complex is not regulated during regeneration by changes in the levels of Osa (S2E-H Fig). Thus, Osa and BAP likely function in parallel to Tara to regulate *en* expression and cell fate during regeneration.

Discussion

To address the question of how regeneration genes are regulated in response to tissue damage, we investigated the roles of PcG and TrxG chromatin modifiers. While previous work has suggested that chromatin modifiers can regulate regeneration [6–17], we took a systematic approach and screened a collection of mutants and RNAi lines that affect a significant number of the chromatin regulators in *Drosophila*. Most of these mutants had regeneration phenotypes, confirming that these genes are important for both promoting and constraining regeneration and likely facilitate the shift from the normal developmental program to the regeneration program, and back again. Most PcG mutants regenerated better than controls, while reduction of TrxG gene expression levels caused varying phenotypes. The dynamic interplay among PcG and TrxG members in regeneration merits future investigation. Here we focused on the role of the SWI/SNF chromatin remodeling

complexes in regulating specific aspects of regeneration. Previous work has provided evidence that SWI/SNF complexes regulate regeneration in other contexts [6],[8]. Here we show that both *Drosophila* SWI/SNF complexes play essential but distinct roles during epithelial regeneration, controlling multiple aspects of the process, including growth, developmental timing, and cell fate. Furthermore, our work has identified multiple likely targets, including *myc*, *ilp8*, and *en*.

Is the requirement for the SWI/SNF complexes for growth and cell fate in the wing disc specific to regeneration? In contrast to *tara,* which is required for posterior wing fate only after damage and regeneration [20], loss of *mor* in homozygous clones during wing disc development caused loss of *en* expression in the posterior compartment [46], although this result was interpreted to mean that *mor* promotes rather than constrains *en* expression. Furthermore, undamaged *mor* heterozygous mutant animals did not show patterning defects (data not shown), while damaged heterozygous mutant animals did (Fig 3E), indicating that regenerating tissue is more sensitive to reductions in SWI/SNF levels than normally developing tissue. By contrast, *osa* is required for normal wing growth[34], but reduction of *osa* levels did not compromise growth during regeneration; instead, PBAP is important for regenerative growth. Thus, some functions of SWI/SNF during regeneration may be the same as during development, although damaged tissue has a heightened

sensitivity to loss of SWI/SNF activity, while other functions of SWI/SNF are unique to regeneration.

SWI/SNF complexes help organisms respond rapidly to stressful conditions or changes in the environment. For example SWI/SNF is recruited by the transcription factor DAF-16/FOXO to promote stress resistance in *Caenorhabditis elegans* [47], and the *Drosophila* BAP complex is required for the activation of target genes of the NF-κB signaling transcription factor Relish in immune responses[48]. Here we show that the *Drosophila* PBAP complex is similarly required for activation of target genes of the JNK signaling transcription factor AP-1 after tissue damage. Indeed, the BAF60a subunit, a mammalian homolog of *Drosophila* BAP60, directly binds the AP-1 transcription factor and stimulates the DNA binding activity of AP-1 [49], suggesting that this role may be conserved.

Future identification of all genes targeted by BAP and PBAP after tissue damage, the factors that recruit these chromatin-remodeling complexes, and the changes they induce at these loci will deepen our understanding of how unexpected or stressful conditions lead to rapid activation of the appropriate genes.

Materials and Methods

Fly stocks

The following fly stocks were obtained for this study. In some cases they were rebalanced before performing experiments: *w^{1118};; rnGAL4, UAS-rpr, tub-GAL80^{ts}/TM6B, tubGAL80* [19], *w^{1118}* (Wild type), *w^{*}; P{neoFRT}82B osa^{308}/TM6B, Tb^{1}* (Bloomington *Drosophila* stock center, BL#5949) [50], *w^{*}; Bap170$^{\Delta 135}$/T(2;3)SM6a-TM6B, Tb^{1}* was a gift from Jessica E. Treisman [51], *brm^{2} e^{s} ca^{1}/TM6B, Sb^{1} Tb^{1} ca^{1}* (BL#3619) [37], *mor^{1}/TM6B, Tb^{1}* (BL#3615) [37], *y^{1} w^{1}; P{neoFRT}40A P{FRT(w^{hs})}G13 cn^{1} PBac{SAstopDsRed}Bap55^{LL05955} bw^{1}/CyO, bw^{1}* (BL#34495) [52], *bap111* RNAi (Vienna *Drosophila* Resource Center, VDRC#104361), *bap60* RNAi (VDRC#12673), *brm* RNAi (VDRC#37721), *P{PZ}tara^{03881} ry^{506}/TM3, ry^{RK} Sb^{1} Ser^{1}* (BL#11613) [53], *UAS-tara* was a gift from Michael Cleary[54], *TRE-Red* was a gift from Dirk Bohmann [45]. A list of the mutants and RNA interference lines used for PcG and TrxG screen can be found in S1 Table. *mor^{12}* allele was a gift from James Kennison [55], *snr1^{E2}* and *snr1^{SR21}* alleles were gifts from Andrew Dingwall [56].

Genetic screen

Mutants or RNAi lines were crossed to *w^{1118};; rnGAL4, UAS-rpr, tubGAL80^{ts}/TM6B, tubGAL80* flies. Embryos were collected at room temperature on grape plates for

4 hours in the dark, then kept at 18°C. Larvae were picked at 2 days after egg lay into standard Bloomington cornmeal media and kept at 18°C, 50 larvae in each vial, 3 vials per genotype per replicate. On day 7, tissue ablation was conducted through a thermal shift to 30°C for 24 hours. Then ablation was stopped by placing the vials in ice water for 60 seconds and returning them to 18°C for regeneration. The regeneration index was calculated by summing the product of wing size and the corresponding percentage of wings for each approximate wing size (0%, 25%, 50%, 75% and 100%). The Δ Index was calculated by subtracting the regeneration index of the control from the regeneration index of the mutant or RNAi line.

To observe and quantify the patterning features and absolute wing size, adult wings were mounted in Gary's Magic Mount (Canada balsam (Sigma) dissolved in methyl salicylate (Sigma)). The mounted adult wings were imaged with an Olympus SZX10 microscope using an Olympus DP21 camera, with the Olympus CellSens Dimension software. Wings were measured using ImageJ.

Immunostaining

Immunostaining was carried out as previously described [19]. Primary antibodies used in this study were rabbit anti-Myc (1:500; Santa Cruz), mouse anti-Nubbin

(1:250; gift from Steve Cohen) [57], mouse anti-engrailed/invected (1:3; Developmental Studies Hybridoma Bank) [58], mouse anti-Patched (1:50; DSHB) [59], mouse anti-Achaete (1:10; DSHB) [60], rabbit anti-PH3 (1:500; Millipore), mouse anti-Osa (1:1; DSHB) [50], rat anti-Ci (1:10; DSHB) [61], rabbit anti-cleaved Caspase-3 (1:200; Cell Signaling), mouse anti-βgal (1:100; DSHB), rabbit anti-phospho-JNK (1:100, Santa Cruz Biotechnology). The Developmental Studies Hybridoma Bank (DSHB) was created by the NICHD of the NIH and is maintained at the University of Iowa, Department of Biology, Iowa City, IA 52242. Secondary antibodies used in this study were AlexaFluor secondary antibodies (Molecular Probes) (1:1000). TO-PRO-3 iodide (Molecular Probes) was used to detect DNA at 1:500.

Confocal images were collected with a Zeiss LSM700 Confocal Microscope using ZEN software (Zeiss). Images were processed with ImageJ (NIH) and Photoshop (Adobe). Average fluorescence intensity was measured by ImageJ. The size of the regenerating wing primordium area was quantified by measuring the anti-Nubbin immunostained area in ImageJ.

Quantitative RT-PCR

qPCR was conducted as previously described [17]. Each independent sample consisted of 30 wing discs. 3 biological replicates were collected for each genotype and time point. Expression levels were normalized to the control *gapdh2*. The fold changes compared to the w^{1118} undamaged wing discs are shown. Primers used in the study were: *GAPDH2* (Forward: 5'-GTGAAGCTGATCTCTTGGTACGAC-3'; Reverse: 5'-CCGCGCCCTAATCTTTAACTTTTAC-3'), and *ilp8* (Forward: 5'-AGTTCGCGATGGAGGCGTGC-3'; Reverse: 5'-TGTGCGTTTTGCCGGATCCAAGT-3').

Pupariation timing experiments

To quantify the pupariation rates, new pupal cases in the vials were counted in 24-hour intervals starting from the end of tissue ablation until no new pupal cases formed. Three independent biological replicates, which consisted of 3 vials each with 50 animals per vial, were performed for each experiment.

Data Availability

All relevant data are available from the authors.

Acknowledgements

The authors would like to thank A. Brock and K. Schuster for critical reading of the

manuscript and helpful discussions; A. Dingwall, D. Bohmann, J. Kennison, J. Treisman, M Cleary, S. Cohen, the Bloomington Drosophila Stock Center (NIH P40OD018537), the Vienna *Drosophila* Resource Center, and the Developmental Studies Hybridoma Bank for fly stocks and reagents.

Funding Sources

This work was supported by a Young Investigator Award from the Roy J. Carver Charitable Trust (#12-4041) (https://www.carvertrust.org) to R.K.S.-B., and a grant from the Nation Institutes of Health (NIGMS R01GM107140) (https://www.nigms.nih.gov) to R.K.S.-B. The funders had no role in study design, data collection and analysis, decision to publish, or preparation of the manuscript.

Author Contributions

Y.T and R.K.S.-B. designed and interpreted the experiments. Y.T carried out all experiments. Y.T and R.K.S.-B. wrote the manuscript.

References

1. Hariharan, I.K., and Serras, F. (2017). Imaginal disc regeneration takes flight. Curr. Opin. Cell Biol. *48*, 10–16.

2. Weintraub, H., and Groudine, M. (1976). Chromosomal subunits in active genes have an altered conformation. Science *193*, 848–856.

3. Wu, C., and Gilbert, W. (1981). Tissue-specific exposure of chromatin structure at the 5' terminus of the rat preproinsulin II gene. Proc. Natl. Acad. Sci. U. S. A. *78*, 1577–1580.

4. McGhee, J.D., Wood, W.I., Dolan, M., Engel, J.D., and Felsenfeld, G. (1981). A 200 base pair region at the 5′ end of the chicken adult β-globin gene is accessible to nuclease digestion. Cell *27*, 45–55.

5. Kouzarides, T. (2007). Chromatin Modifications and Their Function. Cell *128*, 693–705.

6. Jin, Y., Xu, J., Yin, M.-X., Lu, Y., Hu, L., Li, P., Zhang, P., Yuan, Z., Ho, M.S., Ji, H., *et al.* (2013). Brahma is essential for Drosophila intestinal stem cell proliferation and regulated by Hippo signaling. Elife *2*, e00999.

7. Xiong, Y., Li, W., Shang, C., Chen, R.M., Han, P., Yang, J., Stankunas, K., Wu, B., Pan, M., Zhou, B., *et al.* (2013). Brg1 Governs a Positive Feedback Circuit in the Hair Follicle for Tissue Regeneration and Repair. Dev. Cell *25*, 169–181.

8. Sun, X., Chuang, J.-C., Kanchwala, M., Wu, L., Celen, C., Li, L., Liang, H., Zhang, S., Maples, T., Nguyen, L.H., *et al.* (2016). Suppression of the SWI/SNF Component Arid1a Promotes Mammalian Regeneration. Cell Stem Cell *18*, 456–466.

9. Pfefferli, C., Müller, F., Jaźwińska, A., and Wicky, C. (2014). Specific NuRD components are required for fin regeneration in zebrafish. BMC Biol. *12*, 1.

10. Scimone, M.L., Meisel, J., and Reddien, P.W. (2010). The Mi-2-like Smed-CHD4 gene is required for stem cell differentiation in the planarian Schmidtea mediterranea. Development *137*, 1231–1241.

11. Blanco, E., Ruiz-Romero, M., Beltran, S., Bosch, M., Punset, A., Serras, F., and Corominas, M. (2010). Gene expression following induction of regeneration in Drosophila wing imaginal discs. Expression profile of regenerating wing discs. BMC Dev. Biol. *10*, 94.

12. Tseng, A.-S., Carneiro, K., Lemire, J.M., and Levin, M. (2011). HDAC Activity Is Required during Xenopus Tail Regeneration. PLOS ONE *6*, e26382.

13. Fukuda, A., Morris, J.P., and Hebrok, M. (2012). Bmi1 Is Required for Regeneration of the Exocrine Pancreas in Mice. Gastroenterology *143*, 821–831.e2.

14. Stewart, S., Tsun, Z.-Y., and Izpisua Belmonte, J.C. (2009). A histone demethylase is necessary for regeneration in zebrafish. Proc. Natl. Acad. Sci. U. S. A. *106*, 19889–19894.

15. Jin, J., Hong, I.-H., Lewis, K., Iakova, P., Breaux, M., Jiang, Y., Sullivan, E., Jawanmardi, N., Timchenko, L., and Timchenko, N.A. (2015). Cooperation of C/EBP family proteins and chromatin remodeling proteins is essential for termination of liver regeneration. Hepatology *61*, 315–325.

16. Wang, G.-L., Salisbury, E., Shi, X., Timchenko, L., Medrano, E.E., and Timchenko, N.A. (2008). HDAC1 cooperates with C/EBPalpha in the inhibition of liver proliferation in old mice. J. Biol. Chem. *283*, 26169–26178.

17. Skinner, A., Khan, S.J., and Smith-Bolton, R.K. (2015). Trithorax regulates systemic signaling during *Drosophila* imaginal disc regeneration. Development *142*, 3500–3511.

18. Harris, R.E., Setiawan, L., Saul, J., and Hariharan, I.K. (2016). Localized epigenetic silencing of a damage-activated WNT enhancer limits regeneration in mature Drosophila imaginal discs. Elife *5*, e11588.

19. Smith-Bolton, R.K., Worley, M.I., Kanda, H., and Hariharan, I.K. (2009). Regenerative Growth in Drosophila Imaginal Discs Is Regulated by Wingless and Myc. Dev. Cell *16*, 797–809.

20. Schuster, K.J., and Smith-Bolton, R.K. (2015). Taranis Protects Regenerating Tissue from Fate Changes Induced by the Wound Response in Drosophila. Dev. Cell *34*, 119–128.

21. Brock, A.R., Seto, M., and Smith-Bolton, R.K. (2017). Cap-n-collar Promotes Tissue Regeneration by Regulating ROS and JNK Signaling in the *Drosophila* Wing Imaginal Disc. Genetics, genetics.116.196832.

22. Wilson, B.G., and Roberts, C.W.M. (2011). SWI/SNF nucleosome remodellers and cancer. Nat. Rev. Cancer *11*, 481–492.

23. Côté, J., Quinn, J., Workman, J.L., and Peterson, C.L. (1994). Stimulation of GAL4 derivative binding to nucleosomal DNA by the yeast SWI/SNF complex. Science *265*, 53–60.

24. Kwon, H., Imbalzano, A.N., Khavari, P.A., Kingston, R.E., and Green, M.R. (1994). Nucleosome disruption and enhancement of activator binding by a human

SW1/SNF complex. Nature *370*, 477–481.

25. Mohrmann, L., Langenberg, K., Krijgsveld, J., Kal, A.J., Heck, A.J.R., and Verrijzer, C.P. (2004). Differential Targeting of Two Distinct SWI/SNF-Related Drosophila Chromatin-Remodeling Complexes. Mol. Cell. Biol. *24*, 3077–3088.

26. Hargreaves, D.C., and Crabtree, G.R. (2011). ATP-dependent chromatin remodeling: genetics, genomics and mechanisms. Cell Res. *21*, 396–420.

27. Collins, R.T., and Treisman, J.E. (2000). Osa-containing Brahma chromatin remodeling complexes are required for the repression of wingless target genes. Genes Dev. *14*, 3140–3152.

28. Chalkley, G.E., Moshkin, Y.M., Langenberg, K., Bezstarosti, K., Blastyak, A., Gyurkovics, H., Demmers, J.A.A., and Verrijzer, C.P. (2008). The Transcriptional Coactivator SAYP Is a Trithorax Group Signature Subunit of the PBAP Chromatin Remodeling Complex. Mol. Cell. Biol. *28*, 2920–2929.

29. Collins, R.T., Furukawa, T., Tanese, N., and Treisman, J.E. (1999). Osa associates with the Brahma chromatin remodeling complex and promotes the activation of some target genes. EMBO J. *18*, 7029–7040.

30. Vázquez, M., Moore, L., and Kennison, J.A. (1999). The trithorax group gene osa encodes an ARID-domain protein that genetically interacts with the brahma chromatin-remodeling factor to regulate transcription. Development *126*, 733–742.

31. Skeath, J.B., and Carroll, S.B. (1991). Regulation of achaete-scute gene expression and sensory organ pattern formation in the Drosophila wing. Genes Dev. *5*, 984–995.

32. Eaton, S., and Kornberg, T.B. (1990). Repression of ci-D in posterior compartments of Drosophila by engrailed. Genes Dev. *4*, 1068–1077.

33. Phillips, R.G., Roberts, I.J., Ingham, P.W., and Whittle, J.R. (1990). The Drosophila segment polarity gene patched is involved in a position-signalling mechanism in imaginal discs. Development *110*, 105–114.

34. Terriente-Félix, A., and de Celis, J.F. (2009). Osa, a subunit of the BAP chromatin-remodelling complex, participates in the regulation of gene expression in response to EGFR signalling in the Drosophila wing. Dev. Biol. *329*, 350–361.

35. Rendina, R., Strangi, A., Avallone, B., and Giordano, E. (2010). Bap170, a

Subunit of the Drosophila PBAP Chromatin Remodeling Complex, Negatively Regulates the EGFR Signaling. Genetics *186*, 167–181.

36. Moshkin, Y.M., Mohrmann, L., van Ijcken, W.F.J., and Verrijzer, C.P. (2007). Functional differentiation of SWI/SNF remodelers in transcription and cell cycle control. Mol. Cell. Biol. *27*, 651–661.

37. Kennison, J.A., and Tamkun, J.W. (1988). Dosage-dependent modifiers of polycomb and antennapedia mutations in Drosophila. Proc. Natl. Acad. Sci. *85*, 8136–8140.

38. Nagl, N.G., Zweitzig, D.R., Thimmapaya, B., Beck, G.R., and Moran, E. (2006). The *c-myc* Gene Is a Direct Target of Mammalian SWI/SNF–Related Complexes during Differentiation-Associated Cell Cycle Arrest. Cancer Res. *66*, 1289–1293.

39. Colombani, J., Andersen, D.S., and Léopold, P. (2012). Secreted Peptide Dilp8 Coordinates Drosophila Tissue Growth with Developmental Timing. Science *336*, 582–585.

40. Garelli, A., Gontijo, A.M., Miguela, V., Caparros, E., and Dominguez, M. (2012). Imaginal Discs Secrete Insulin-Like Peptide 8 to Mediate Plasticity of Growth and Maturation. Science *336*, 579–582.

41. Becker, P.B., and Workman, J.L. (2013). Nucleosome Remodeling and Epigenetics. Cold Spring Harb. Perspect. Biol. *5*, a017905–a017905.

42. Bergantinos, C., Corominas, M., and Serras, F. (2010). Cell death-induced regeneration in wing imaginal discs requires JNK signalling. Development *137*, 1169–1179.

43. Bosch, M., Bagun, J., and Serras, F. (2008). Origin and proliferation of blastema cells during regeneration of Drosophila wing imaginal discs. Int. J. Dev. Biol. *52*, 1043–1050.

44. Perkins, K.K., Dailey, G.M., and Tjian, R. (1988). Novel Jun-and Fos-related proteins in Drosophila are functionally homologous to enhancer factor AP-1. EMBO J. *7*, 4265.

45. Chatterjee, N., and Bohmann, D. (2012). A Versatile ΦC31 Based Reporter System for Measuring AP-1 and Nrf2 Signaling in Drosophila and in Tissue Culture. PLoS ONE *7*, e34063.

46. Brizuela, B.J., and Kennison, J.A. (1997). The Drosophila homeotic gene moira regulates expression of engrailed and HOM genes in imaginal tissues. Mech. Dev. *65*, 209–220.

47. Riedel, C.G., Dowen, R.H., Lourenco, G.F., Kirienko, N.V., Heimbucher, T., West, J.A., Bowman, S.K., Kingston, R.E., Dillin, A., Asara, J.M., *et al.* (2013). DAF-16 employs the chromatin remodeller SWI/SNF to promote stress resistance and longevity. Nat. Cell Biol. *15*, 491–501.

48. Bonnay, F., Nguyen, X.-H., Cohen-Berros, E., Troxler, L., Batsche, E., Camonis, J., Takeuchi, O., Reichhart, J.-M., and Matt, N. (2014). Akirin specifies NF- B selectivity of Drosophila innate immune response via chromatin remodeling. EMBO J. *33*, 2349–2362.

49. Ito, T., Yamauchi, M., Nishina, M., Yamamichi, N., Mizutani, T., Ui, M., Murakami, M., and Iba, H. (2001). Identification of SWI·SNF Complex Subunit BAF60a as a Determinant of the Transactivation Potential of Fos/Jun Dimers. J. Biol. Chem. *276*, 2852–2857.

50. Treisman, J.E., Luk, A., Rubin, G.M., and Heberlein, U. (1997). eyelidantagonizes wingless signaling during Drosophiladevelopment and has homology to the Bright family of DNA-binding proteins. Genes Dev. *11*, 1949–1962.

51. Carrera, I., Zavadil, J., and Treisman, J.E. (2008). Two Subunits Specific to the PBAP Chromatin Remodeling Complex Have Distinct and Redundant Functions during Drosophila Development. Mol. Cell. Biol. *28*, 5238–5250.

52. Schuldiner, O., Berdnik, D., Levy, J.M., Wu, J.S., Luginbuhl, D., Gontang, A.C., and Luo, L. (2008). piggyBac-Based Mosaic Screen Identifies a Postmitotic Function for Cohesin in Regulating Developmental Axon Pruning. Dev. Cell *14*, 227–238.

53. Gutierrez, L. (2003). The Drosophila trithorax group gene tonalli(tna) interacts genetically with the Brahma remodeling complex and encodes an SP-RING finger protein. Development *130*, 343–354.

54. Manansala, M.C., Min, S., and Cleary, M.D. (2013). The Drosophila SERTAD protein Taranis determines lineage-specific neural progenitor proliferation patterns. Dev. Biol. *376*, 150–162.

55. Kennison, J.A., and Tamkun, J.W. (1988). Dosage-dependent modifiers of polycomb and antennapedia mutations in Drosophila. Proc. Natl. Acad. Sci. *85*, 8136–

8140.

56. Zraly, C.B., Marenda, D.R., Nanchal, R., Cavalli, G., Muchardt, C., and Dingwall, A.K. (2003). SNR1 is an essential subunit in a subset of Drosophila brm complexes, targeting specific functions during development. Dev. Biol. *253*, 291–308.

57. Ng, M., Diaz-Benjumea, F.J., Vincent, J.-P., Wu, J., and Cohen, S.M. (1996). Specification of the wing by localized expression of wingless protein. Nature *381*, 316–318.

58. Patel, N.H., Martin-Blanco, E., Coleman, K.G., Poole, S.J., Ellis, M.C., Kornberg, T.B., and Goodman, C.S. (1989). Expression of engrailed proteins in arthropods, annelids, and chordates. Cell *58*, 955–968.

59. Capdevila, J., Estrada, M.P., Sánchez-Herrero, E., and Guerrero, I. (1994). The Drosophila segment polarity gene patched interacts with decapentaplegic in wing development. EMBO J. *13*, 71–82.

60. Skeath, J.B., and Carroll, S.B. (1992). Regulation of proneural gene expression and cell fate during neuroblast segregation in the Drosophila embryo. Dev. Camb. Engl. *114*, 939–946.

61. Motzny, C.K., and Holmgren, R. (1995). The Drosophila cubitus interruptus protein and its role in the wingless and hedgehog signal transduction pathways. Mech. Dev. *52*, 137–150.

Figure 1

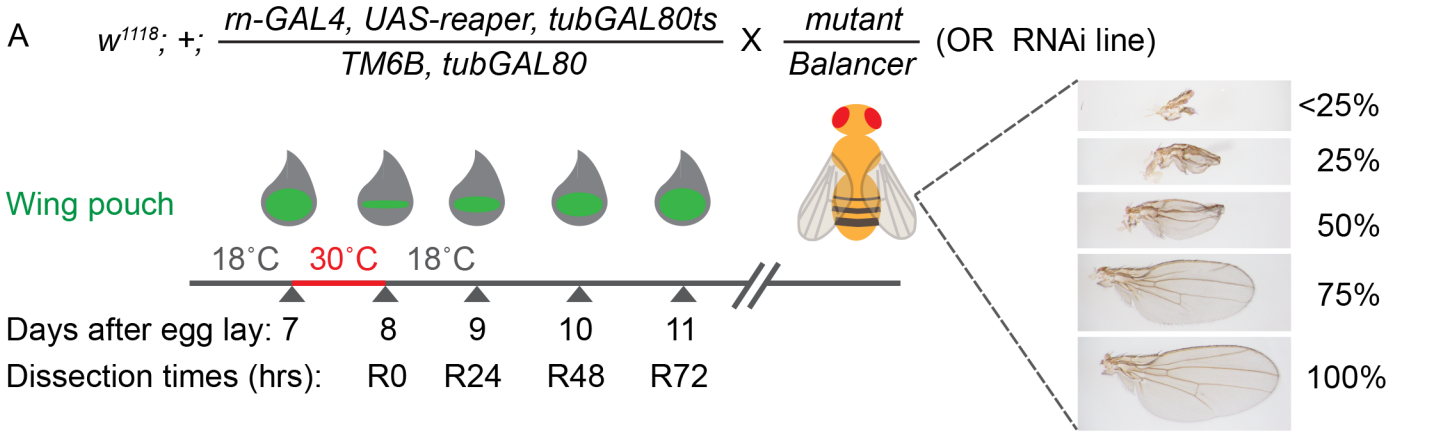
A
w1118; +; rn-GAL4, UAS-reaper, tubGAL80ts / TM6B, tubGAL80 X mutant / Balancer (OR RNAi line)
Wing pouch
18˚C
30˚C
18˚C
Days after egg lay: 7 8 9 10 11
Dissection times (hrs): R0 R24 R48 R72
<25%
25%
50%
75%
100%

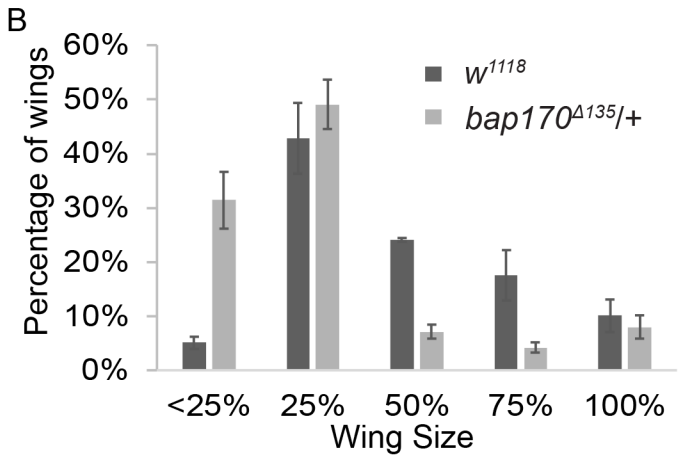
B
Percentage of wings
60%
50%
40%
30%
20%
10%
0%
w1118
bap170Δ135/+
<25%
25%
50%
75%
100%
Wing Size

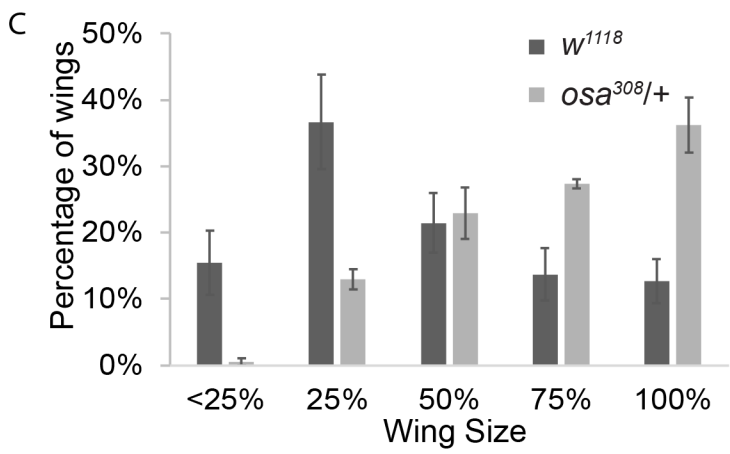
C
Percentage of wings
50%
40%
30%
20%
10%
0%
w1118
osa308/+
<25%
25%
50%
75%
100%
Wing Size

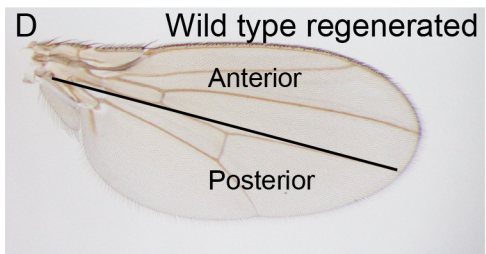
D
Wild type regenerated
Anterior
Posterior

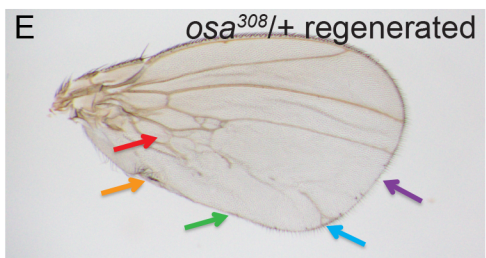
E
osa308/+ regenerated

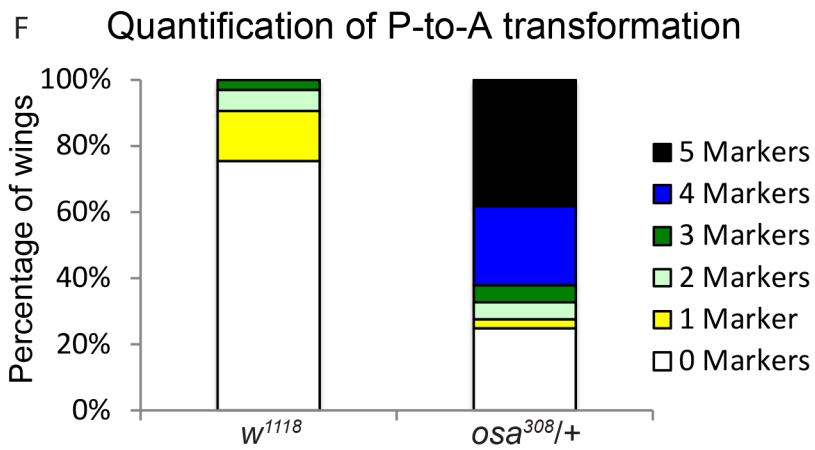
F
Quantification of P-to-A transformation
Percentage of wings
100%
80%
60%
40%
20%
0%
w1118
osa308/+
5 Markers
4 Markers
3 Markers
2 Markers
1 Marker
0 Markers

Fig 1. SWI/SNF components Bap170 and Osa are required for regeneration

(A) Method for screening mutants or RNAi lines using a genetic ablation system. Mutants or RNAi lines of PcG and TrxG genes were crossed to the ablation system (*w*^{1118}*; +; rn-GAL4, UAS-rpr, tubGAL80*^{ts}*/TM6B, tubGAL80*). Animals were kept at 18°C until 7 days after egg lay (AEL). Then they were moved to 30°C to induce tissue ablation for 24 hours, then back to 18°C to enable recovery (R). The size of the regenerated adult wings was assessed semi-quantitatively by counting the number of wings that were approximately 0%, 25%, 50%, 75% or 100% of the length of a control adult wing with no tissue damage. The regenerating discs were also examined at different times during recovery such as R0, R24, R48 and R72.

(B) Comparison of the size of adult wings after imaginal disc damage and regeneration in *bap170*$^{\Delta 135}$/+ and wild-type (*w*^{1118}) animals. n = 190 wings (*bap170*$^{\Delta 135}$/+) and 406 wings (*w*^{1118}) from 3 independent experiments. Chi-square test $p < 0.001$.

(C) Comparison of the size of adult wings after imaginal disc damage and regeneration in *osa*^{308}/+ and wild-type (*w*^{1118}) animals. n = 146 wings (*osa*^{308}/+) and 296 wings (*w*^{1118}) from three independent experiments. Chi-square test $p < 0.001$.

(D) Wild-type adult wing after disc regeneration. Anterior is up.

(E) *osa*^{308}/+ adult wing after disc regeneration. Arrows show five anterior-specific

markers in the posterior compartment: anterior crossveins (red), alula-like costa bristles (orange), margin vein (green), socketed bristles (blue), and change of wing shape with wider distal portion of the wing, similar to the anterior compartment (purple).

(F) Quantification of the number of Posterior-to-Anterior transformation markers described in (E) in each wing after damage and regeneration of the disc, comparing *osa*^{308}/+ wings to wild-type (*w*^{1118}) wings, n = 51 wings (*osa*^{308}/+) and 45 wings (*w*^{1118}), from 3 independent experiments. Chi-square test $p < 0.001$. Error bars are SEM.

Figure 2

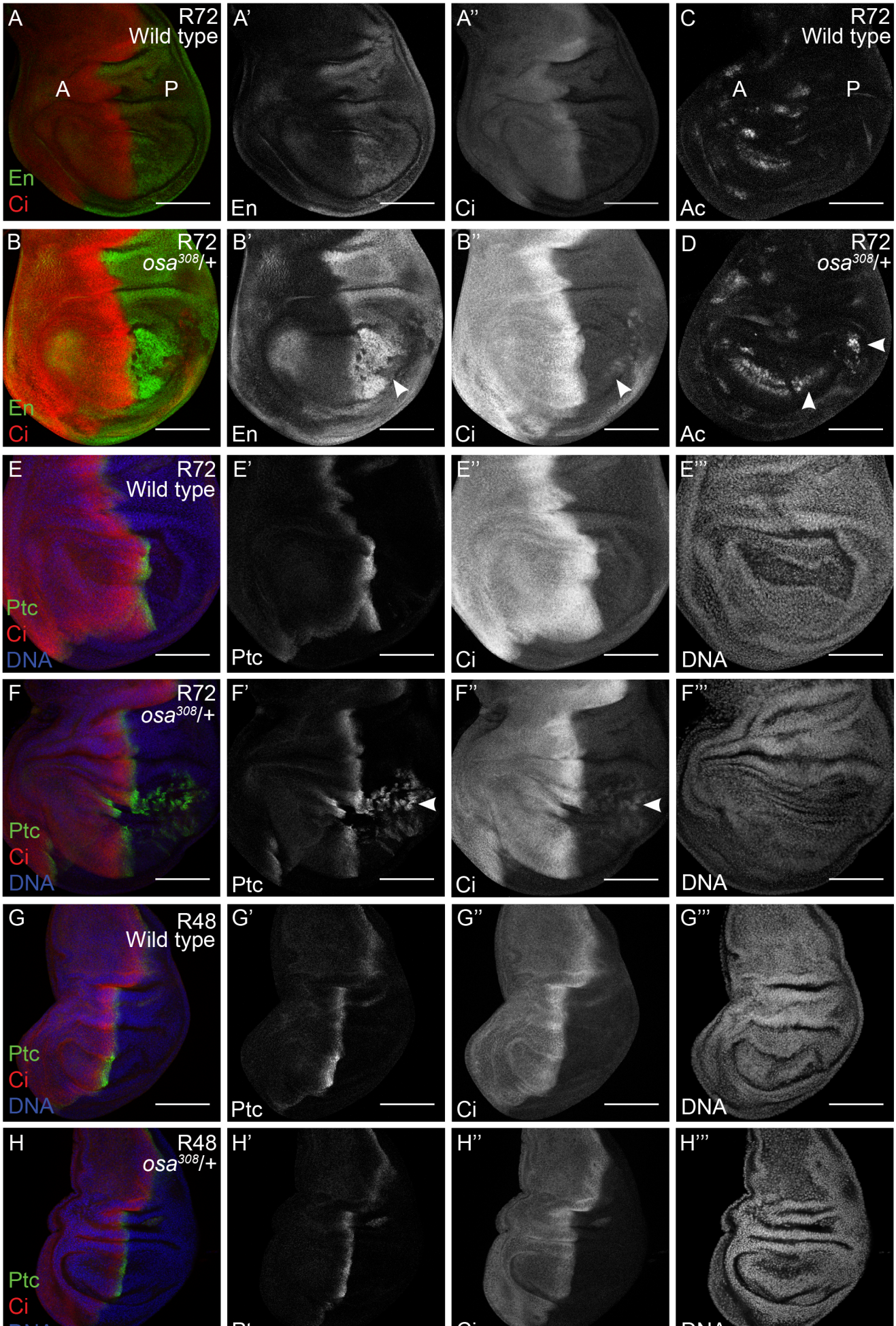

Fig 2. *osa*/+ mutant showed Posterior-to-Anterior transformations during wing disc regeneration

(A) Wild-type (w^{1118}) regenerating wing disc at R72 with En (green) and Ci (red) immunostaining. Anterior is left for all wing disc images.

(B) osa^{308}/+ regenerating wing discs at R72 with En (green) and Ci (red) immunostaining. Arrowhead points to the low En expression region in which Ci is expressed in the posterior compartment.

(C) Wild-type (w^{1118}) regenerating wing disc at R72 with Ac immunostaining.

(D) osa^{308}/+ regenerating wing disc at R72 with Ac immunostaining. Arrowheads show Ac expression in the posterior compartment.

(E) Wild-type (w^{1118}) regenerating wing disc at R72 with Ptc (green) (E') and Ci (red)(E'') immunostaining. DNA (blue)(E''') was detected with Topro3.

(F) osa^{308}/+ regenerating wing disc at R72 with Ptc (green)(F') and Ci (red)(F'') immunostaining. DNA (blue)(F''') was detected with Topro3. Arrowhead shows Ptc and Ci co-expression in the posterior compartment.

(G) Wild-type (w^{1118}) regenerating wing disc at R48 with Ptc (green)(G') and Ci (red)(G'') immunostaining. DNA (blue)(G''') was detected with Topro3.

(H) osa^{308}/+ regenerating wing disc at R48 with Ptc (green)(H') and Ci (red)(H'') immunostaining. DNA (blue)(H''') was detected with Topro3.

Scale bars are 100μm for all wing disc images.

Figure 3

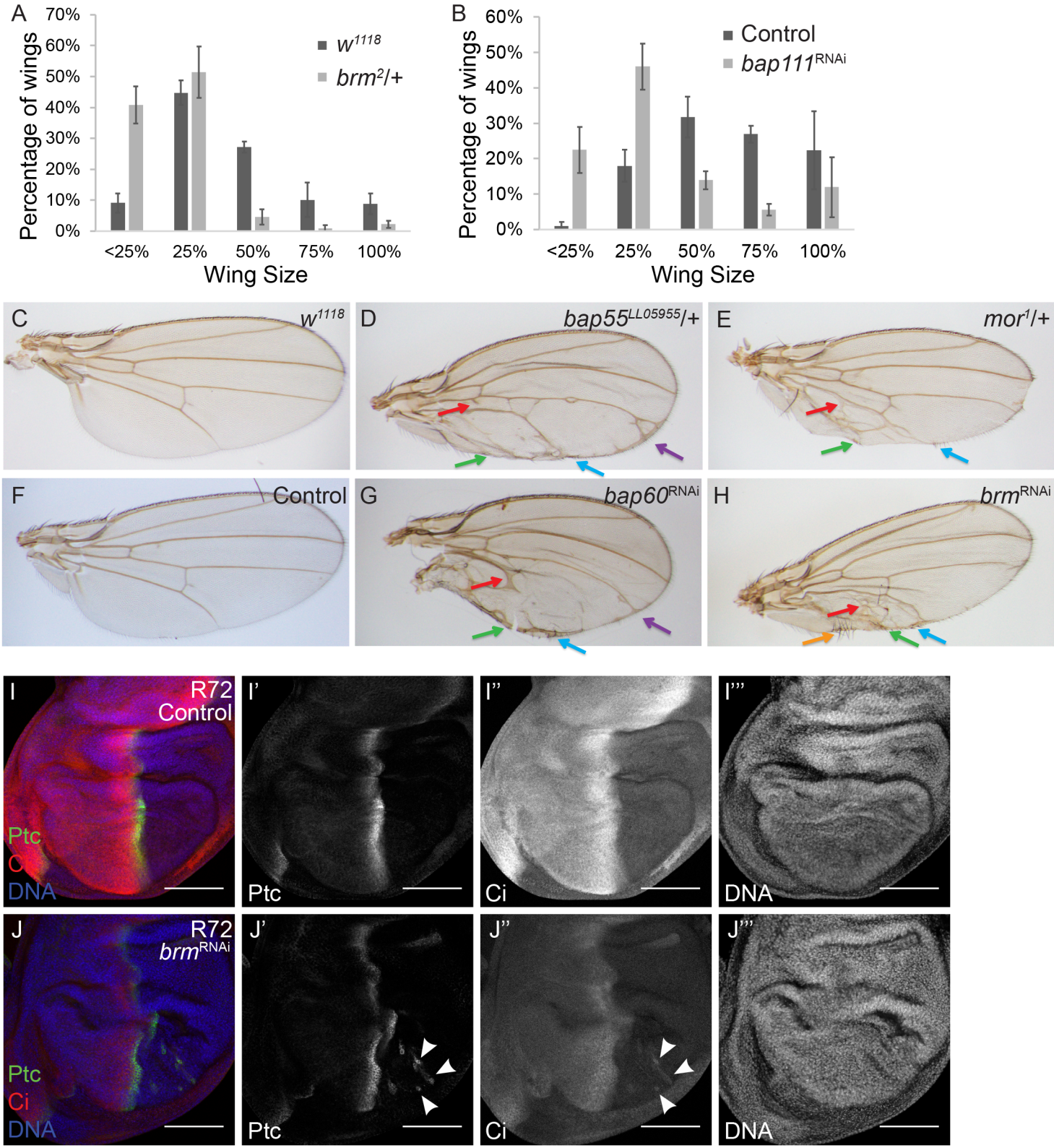
A
Percentage of wings
70%
60%
50%
40%
30%
20%
10%
0%
w1118
brm2/+
<25%
25%
50%
75%
100%
Wing Size
B
Percentage of wings
60%
50%
40%
30%
20%
10%
0%
Control
bap111RNAi
<25%
25%
50%
75%
100%
Wing Size
C
w1118
D
bap55LL05955/+
E
mor1/+
F
Control
G
bap60RNAi
H
brmRNAi
I
R72
Control
Ptc
Ci
DNA
I'
Ptc
I''
Ci
I'''
DNA
J
R72
brmRNAi
Ptc
Ci
DNA
J'
Ptc
J''
Ci
J'''
DNA

Fig 3. SWI/SNF core components are required for both growth and posterior fate during wing disc regeneration

(A) Comparison of the size of adult wings after imaginal disc damage and regeneration in *brm*^{2}/+ and wild-type (*w*^{1118}) animals. n = 142 wings (*brm*^{2}/+) and 224 wings (*w*^{1118}) from 3 independent experiments. Chi-square test $p < 0.001$

(B) Comparison of the size of adult wings after imaginal disc damage and regeneration in animals expressing *bap111* RNAi and control animals. n = 264 wings (*bap111* RNAi) and 291 wings (control) from 3 independent experiments. The control for RNAi lines is VDRC 6000 in all experiments. Chi-square test $p < 0.001$

(C-E) Adult wing after disc regeneration of wild-type (*w*^{1118}) (C), *bap55*^{LL05955}/+ (D) and *mor*^{1}/+ (E). Anterior is up for all adult wing images. Arrows point to anterior features identified in the posterior compartment. Arrows show five anterior-specific markers in the posterior compartment: anterior crossveins (red), alula-like costa bristles (orange), margin vein (green), socketed bristles (blue), and change of wing shape with wider distal portion of the wing, similar to the anterior compartment (purple).

(F-H) Adult wing after disc regeneration of animals expressing control, *bap60* RNAi (G) and *brm* RNAi (H).

(I) Control regenerating wing disc at R72 with Ptc (green) (I') and Ci (red) (I'') immunostaining. DNA (blue) (I''') was detected with Topro3.

(J) Regenerating wing disc of animals expressing *brm* RNAi at R72 with Ptc (green) (J') and Ci (red) (J'') immunostaining. DNA (blue) (J''') was detected with Topro3. Arrowheads show Ptc and Ci co-expression in the posterior compartment.

Error bars are SEM. Scale bars are 100μm for all wing discs images.

Figure 4

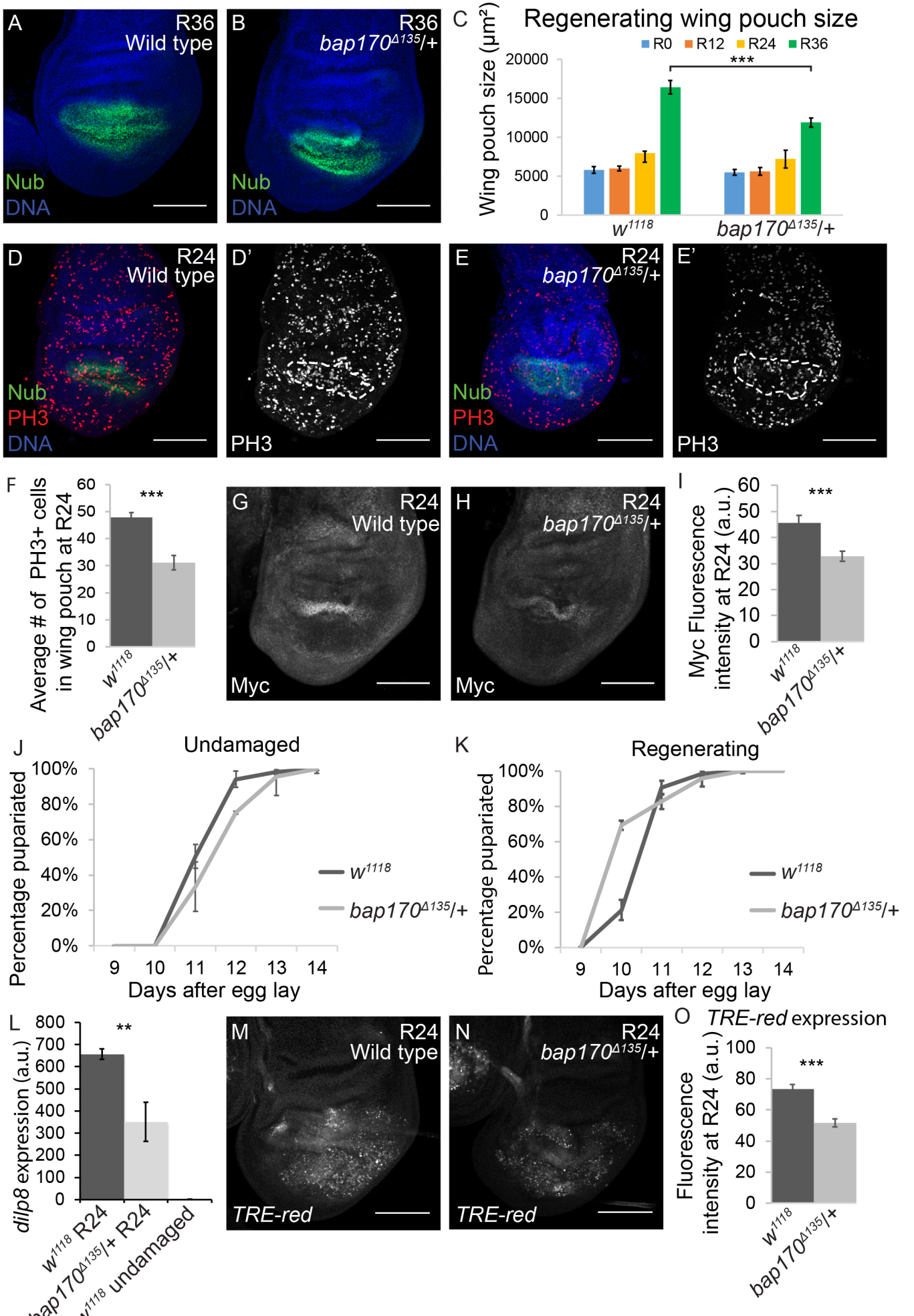

Fig 4. Decreased *bap170* expression limits regenerative growth and pupariation delay

(A) Wild-type (w^{1118}) regenerating wing disc at R36 with wing pouch marked by anti-Nubbin (green) immunostaining. DNA (blue) was detected with Topro3.

(B) $bap170^{\Delta 135}$/+ regenerating wing disc at R36 with wing pouch marked by anti-Nubbin (green) immunostaining. DNA (blue) was detected with Topro3.

(C) Comparison of regenerating wing pouch size at 0, 12, 24, 36 hours after imaginal disc damage and regeneration in $bap170^{\Delta 135}$/+ and wild-type (w^{1118}) animals.

(D-E) Regenerating wild-type (w^{1118}) (D) and $bap170^{\Delta 135}$/+ (E) wing discs at R24 with Nubbin (green) and PH3 (red) immunostaining. DNA (blue) was detected with Topro3. Dashed white outline shows the regenerating wing primordium labeled with Nubbin.

(F) Average number of mitotic cells (marked with PH3 immunostaining) in the wing primordium (stained with anti-Nubbin) at R24 in $bap170^{\Delta 135}$/+ and wild-type (w^{1118}) animals. n = 8 wing discs ($bap170^{\Delta 135}$/+) and 10 wing discs (w^{1118}).

(G-H) Wild-type (w^{1118}) (G) and $bap170^{\Delta 135}$/+ (H) regenerating wing discs at R24 with Myc immunostaining.

(I) Quantification of anti-Myc immunostaining fluorescence intensity in the wing pouch in $bap170^{\Delta 135}$/+ and wild-type (w^{1118}) regenerating wing discs at R24. n = 9

wing discs (*bap170*$^{\Delta 135}$/+) and 9 wing discs (*w*^{1118}).

(J) Pupariation rates of animals during normal development at 18°C. n = 121 pupae (*bap170*$^{\Delta 135}$/+) and 245 pupae (*w*^{1118}) from 3 independent experiments.

(K) Pupariation rates of animals after tissue damage (30°C) and regeneration (18°C). n = 117 pupae (*bap170*$^{\Delta 135}$/+) and 231 pupae (*w*^{1118}) from 3 independent experiments. Because the temperature shifts to 30°C in the ablation protocol increase the developmental rate, the pupariation timing of regenerating animals (K) cannot be compared to the undamaged control animals (J).

(L) *ilp8* expression examined by qPCR of *bap170*$^{\Delta 135}$/+ and wild-type (*w*^{1118}) regenerating wing discs at R24. The graph shows fold change relative to wild-type (*w*^{1118}) undamaged discs.

(M-N) Expression of *TRE-Red*, a JNK signaling reporter, in wild-type (*w*^{1118}) (M) and *bap170*$^{\Delta 135}$/+ (N) regenerating wing discs at R24.

(O) Quantification of *TRE-Red* expression fluorescence intensity in *bap170*$^{\Delta 135}$/+ and wild-type (*w*^{1118}) regenerating wing pouches at R24.

Scale bars are 100µm for all wing discs images. * $p < 0.1$, ** $p < 0.05$, *** $p < 0.01$, Student's *t*-test.

Figure 5

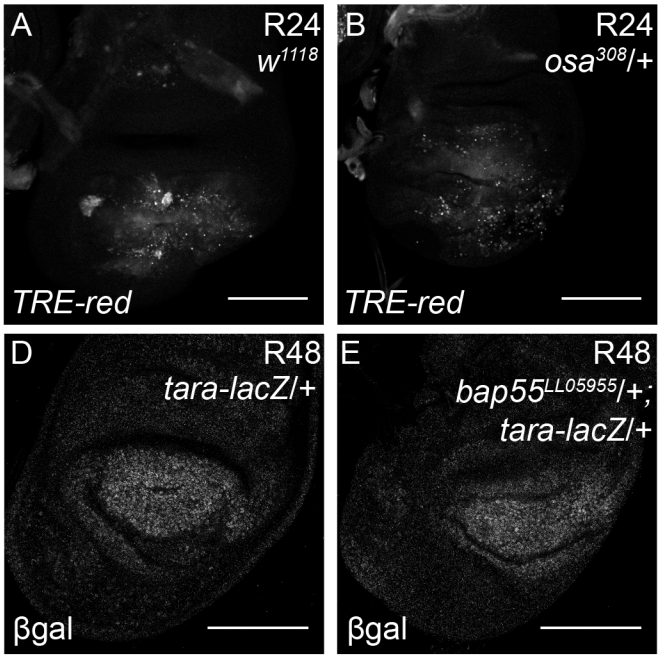
A
R24
w1118
TRE-red
B
R24
osa308/+
TRE-red
D
R48
tara-lacZ/+
βgal
E
R48
bap55LL05955/+;
tara-lacZ/+
βgal

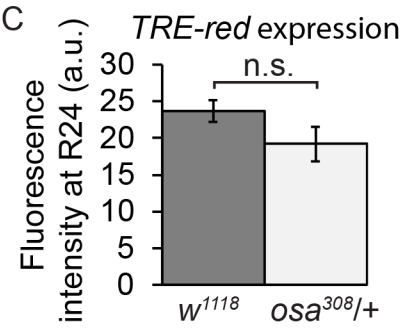
C
TRE-red expression
Fluorescence intensity at R24 (a.u.)
30
25
20
15
10
5
0
n.s.
w1118
osa308/+

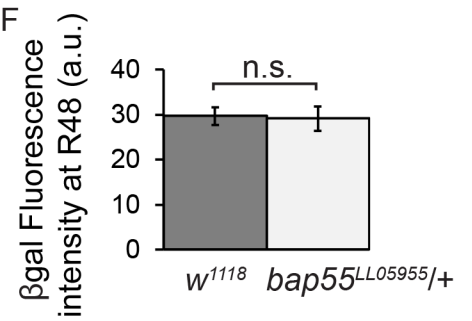
F
βgal Fluorescence intensity at R48 (a.u.)
40
30
20
10
0
n.s.
w1118
bap55LL05955/+


G
w1118


H
osa308/+

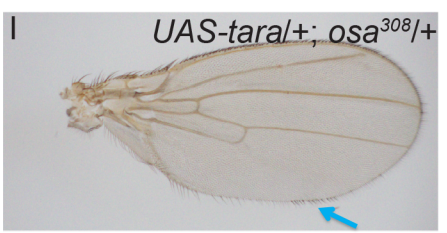
I
UAS-tara/+; osa308/+

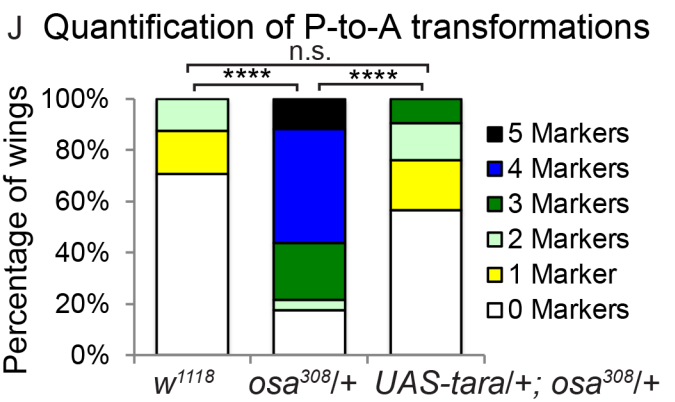
J Quantification of P-to-A transformations
n.s.
****
****
Percentage of wings
100%
80%
60%
40%
20%
0%
5 Markers
4 Markers
3 Markers
2 Markers
1 Marker
0 Markers
w1118
osa308/+
UAS-tara/+; osa308/+

Fig 5. The BAP complex functions in parallel to Tara to prevent P-to-A transformations.

(A-B) Expression of *TRE-Red*, a JNK signaling reporter, in wild-type (w^{1118}) (A) and osa^{308}/+ (B) regenerating wing discs at R24.

(C) Quantification of *TRE-Red* expression fluorescence intensity in osa^{308}/+ and wild-type (w^{1118}) regenerating wing pouches at R24. n = 7 wing discs (osa^{308}/+) and 10 wing discs (w^{1118}). Error bars are SEM.

(D-E) *tara-lacZ*/+ (D) and $bap55^{LL05955}$/+; *tara-lacZ*/+ (E) regenerating wing discs at R48 stained with β-gal.

(F) Quantification of β-gal expression fluorescence intensity in $bap55^{LL05955}$/+ and wild-type (w^{1118}) regenerating wing pouches at R48. n = 8 wing discs ($bap55^{LL05955}$/+) and 9 wing discs (w^{1118}). Error bars are SEM.

(G-I) Adult wing after disc regeneration in wild-type (w^{1118}) (G), osa^{308}/+ (H) and *UAS-tara*/+; osa^{308}/+ (I) animals. Arrows show five anterior-specific markers in the posterior compartment: anterior crossveins (red), alula-like costa bristles (orange), margin vein (green), socketed bristles (blue), and change of wing shape with wider distal portion of the wing, similar to the anterior compartment (purple). Anterior is up for all adult wing images.

(J) Quantification of the number of Posterior-to-Anterior transformation markers described in Fig 1E in each wing after damage and regeneration of the disc,

comparing *UAS-tara*/+; osa^{308}/+ wings to osa^{308}/+ and wild-type (w^{1118}) wings, n = 21 wings (*UAS-tara*/+; osa^{308}/+), n = 16 wings (osa^{308}/+) and n = 34 wings (w^{1118}), from 3 independent experiments. **** $p < 0.0001$, Chi-square test. Chi-square test measuring *UAS-tara*/+; osa^{308}/+ against w^{1118}, $p = 0.86$, not significant. Scale bars are 100µm for all wing discs images. * $p < 0.1$, ** $p < 0.05$, *** $p < 0.01$, Student's *t*-test.